Effects of wind gustiness and air density on the evolution of wave fields

Luigi Cavaleri

Istituto Studio Dinamica Grandi Masse
S.Polo 1364
30125 Venice, Italy
e-mail L.Cavaleri@isdgm.ve.cnr.it

1. The background

The last decade has seen a substantial improvement of the results from meteorological models, both as analysis and forecast. The improvement is due, among other things, to an increased resolution, to a more sophisticated assimilation of the growing amount of measured data, and to an improved description of the basic physical processes that govern the evolution of the atmosphere. All this is evident in the steady decrease of the bias of the physical quantities derived from the models. At the European Centre for Medium-Range Weather Forecasts (ECMWF, Reading, U.K.) the present bias for the analysed surface wind speeds, U_{10}, on the global oceans is of the order of 20-30 cm/s.

This steady improvement is not met with a corresponding decrease of the rms error. In other words, the model characterises well the average properties of the atmosphere, but it is unable to properly represent its short term variability (we will soon characterise these scales). So, for surface wind speed, that will be our basic interest in this paper, the global average scatter index is still close to 0.2. Apart from the determination, in time and space, of a wind field, this has implications also for modelling the processes that receive energy from the atmosphere, wind waves being perhaps the most obvious example. The key factor lies in the nonlinearity that characterise the transfer of energy and momentum from the atmosphere to the ocean. As shown in Komen et al (1994), the effects can be large.

One basic problem is that at present the theory cannot justify the level of short term variability σ found in the atmosphere (Anton Beljaars, personal communication). A realistic σ is crucial as the effects increase rapidly with it. We have analysed the problem hindcasting two long periods, using for the simulation of gustiness measured data taken in the open sea. This is described in the two following sections, where (sect. 2) we describe the gustiness, its representation and its effects on the growth of wind waves. In sect. 3 we deal with the hindcasts and the related results.

Next, we discuss another aspect of the energy transfer between the atmosphere and the ocean, namely the influence of a variable air density ρ_{air}, whose value is usually considered as constant in wave and circulation modelling. In sect. 4 we show the effect of a variable ρ_{air} in some test cases, followed in 5 by two long hindcasts. The overall conclusions and recommendations are drawn in the final sect. 6.

2. Variability in the lower atmosphere and its effects on wave growth

High frequency records of surface wind speed show a substantial variability superimposed to the general trend of the, e.g., hourly mean values. These fluctuations can be characterised as:

a) long term, with a time scale equal to, or longer than, the interval between sequential synoptic times. These are mostly represented in the output of the meteorological models,

b) short term, with period between one minute and a few hours. Independent of the limitations connected to the integration time step, these fluctuations are mostly absent in meteorological modelling,

c) high frequency, with scales from a fraction of a second to one minute. These are not of immediate interest for our present discussion, and will not be considered further in this paper.

An example of the differences between modelled and measured surface wind fields is given in Fig.1, where we see the structure of the two fields along the ground track of the Topex altimeter during a mistral storm in the Western Mediterranean Sea. It is clear that the satellite data (dots) exhibit a variability not represented in the modelled data (circles).

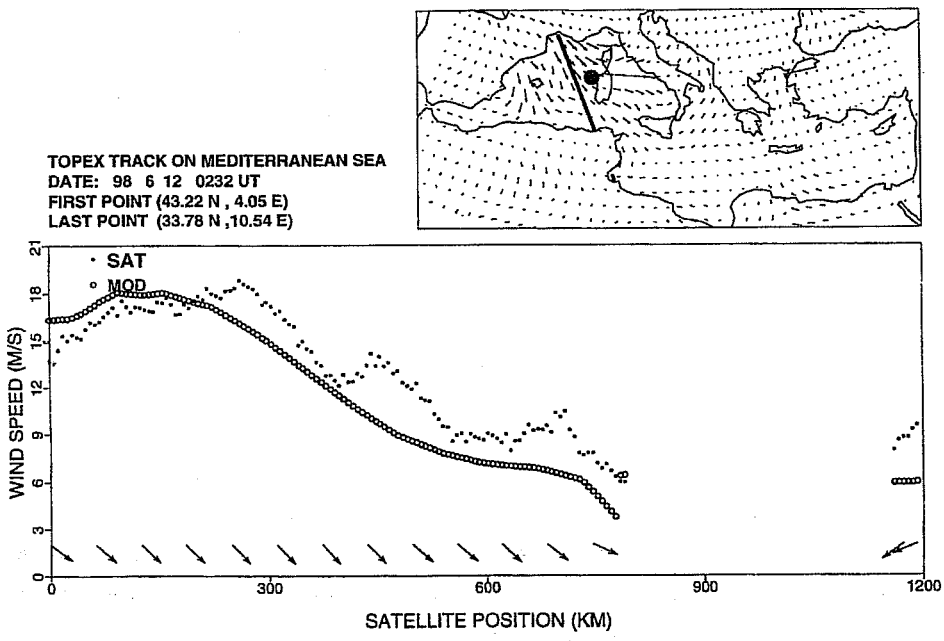

Fig 1 Measured (dots) and model (circles) wind speed along the Topex ground track shown in the small insert. The small dot indicates the position of Alghero.

The lack of variability in the meteorological models is not only a matter of scale. The limited area models go down till scales of the order of kilometres and minutes. However, in general the fluctuations mentioned above in b) are not present or poorly represented. The models tend to smooth these fluctuations, either for numerical or physical reasons. A further limit is given by the interval with which the data are archived, typically three or six hours, that destroys the intermediate information. The operational applications at ECMWF do not have this problem, because the atmospheric and wave models are coupled every time step. However, this is not possible with later hindcasts, that rely on the archived wind fields. The conclusion is that, if we wish to take the wind variability into consideration, we have to resort to its parameterisation, starting from the available information.

Extensive measurement campaigns (see, e.g., Smith et al, 1990) have indicated that, within limited time intervals, the wind speed values from open sea records are Gaussian distributed (we will refer to this variability as gustiness). Moreover, the spectral analysis shows that the highest energy levels are reached in the low frequency range. This corresponds to a degree of persistence around the value present at a certain time, or, in other words, to a coherence between the sequential values. Following Cavaleri and Burgers (1992), the time series have been modelled as

$$b_{i+1} = \alpha b_i + a_{i+1} \tag{1}$$

where **b** is the sought sequence, i the progressive index, α the coherence between sequential values, **a** are random numbers. Fig.2 (from Komen et al, 1994, p.324) shows four time series produced starting from the same values of **a**, but with different coherence.

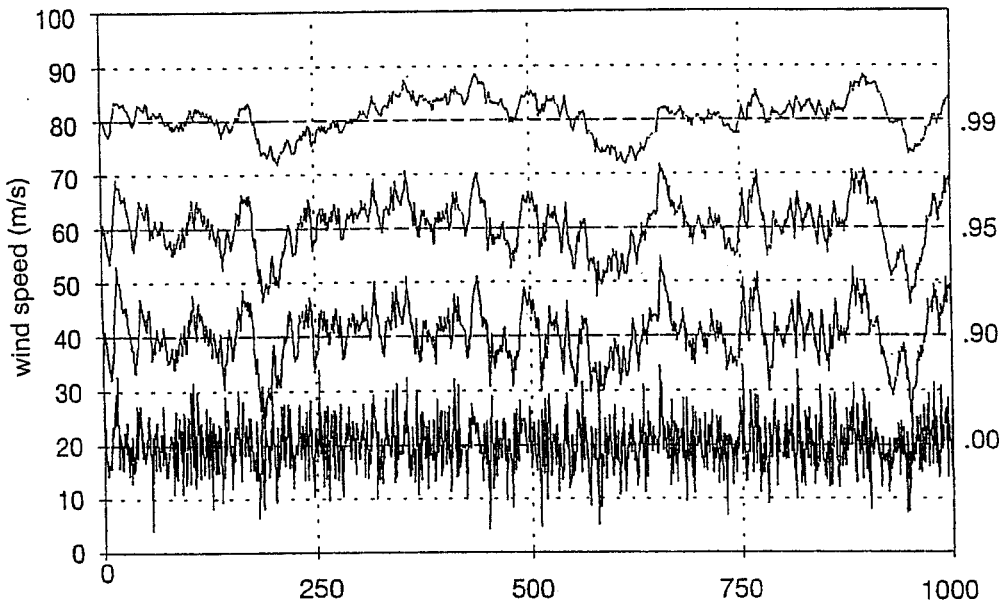

Fig 2 Synthetic time series obtained with the same sequence of random numbers, but with different correlation (shown on the right side) between sequential values (after Komen et al, 1994, p.324).

Fig.3 displays a number of spectra from wind records taken in the open ocean. Superimposed are three spectra from synthetic time series obtained with no coherence between sequential values (α=0, corresponding to a white spectrum), α=0.8 and α=0.9. We see that the value α=0.9 fits well the data, considered at 10 minute interval. Therefore we have assumed this value in our simulation of gustiness with (1).

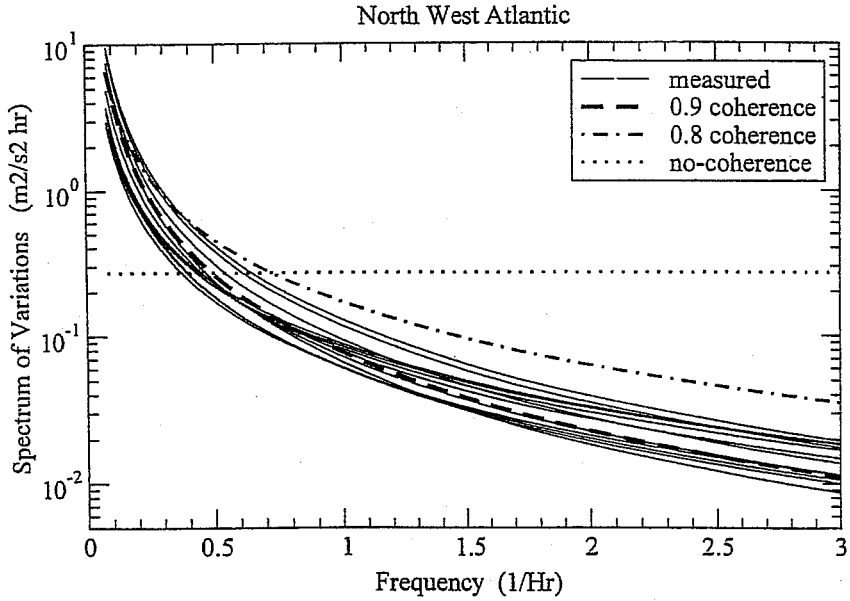

Fig 3 Frequency spectra of wind speeds measured at offshore buoys. The dot, dashed, dash-dot lines indicate spectra from sequences of random numbers with sequential correlation equal to 0., 0.9, 0.8 respectively (see Fig.2).

Granted the time variability of U_{10}, we are still left with the determination of its amplitude. This is a problem, because, as mentioned in the previous section, the present theories do not justify the level of gustiness, up to 30% or more, that we find on the oceans (see, among others, Monahan and Armendariz, 1971, and Sethuraman, 1979). We have two possibilities. One is to accept the present theories, an approach recently implemented at ECMWF (see the communication by Saleh Abdalla in this workshop); the other one, with a more immediate attitude towards practical applications, is to accept a realistic parameterisation of gustiness that we can derive from direct measurements in the open sea. This is the approach we follow in this paper.

A first solution in this direction was provided by Bauer and Weisse (2000), who used some long term measurements taken from a tower in the North Sea to derived realistic wind speed spectra that they superimposed to the linearly interpolated values from the ECMWF archive. Their approach is sophisticated, but it assumes constant characteristics of gustiness σ in space and time. Indeed, practical experience at sea suggests that σ is a rather variable quantity. Relying on experimental data taken from an oceanographic tower located in the Northern Adriatic Sea (Cavaleri, 2000), we have found a relationship between the level of gustiness and the local air-sea temperature difference, expressed by

$$\sigma = \max(0., 0.025(t_{water} - t_{air})) \tag{2}$$

where σ is expressed in adimensional terms. Note that (2) is a crude approximation for limited temperature differences, because a certain level of gustiness is always present. However, small values of σ have no practical implications for wave growth (see Komen et al, 1994, p.322), hence (2) is suitable for our present purposes.

For the practical implementation in a wave model, WAM in our case (WAM-DI Group, 1988), the wind speed is kept constant during the integration time step, typically between 15 and 20 minutes. Each single value is obtained adding to the undisturbed mean U_{10} a fluctuation

$$\Delta = r\,\sigma\,U_{10} \tag{3}$$

where r is a random number with unit variance, generated at each time step. Note that the standard deviation of the **b** sequence in (1), σ_b, is related to that of the random **a** sequence σ_a by (Box and Jenkins, 1970)

$$\sigma_a^2 = (1-\alpha^2)\,\sigma_b^2 \tag{4}$$

The fact that $\sigma_b > \sigma_a$ represents the tendency of the **b**, hence U_{10}, sequence to remain in the range of values present at a certain time.

While (3) provides a realistic representation of the gustiness at sea, for the purpose of practical applications it turns out convenient to consider also two different sequential rules. One is to assume α=0, i.e. no correlation in time. The resulting random number sequence is represented in the lowest diagram of Fig.2. The other approach is to consider a simple flip-flop sequence, i.e. r in (3) takes alternatively the values $\pm$1.

Before discussing practical applications, for a better understanding of the problem it is useful to consider the ideal situation of the one point model. This corresponds to an infinite ocean with a spatially uniform wind. Under a gusty wind waves grow faster and longer for two different reasons. The first, less important one, is the nonlinearity of the friction velocity u_* with respect to U_{10}. This is active since the onset of a storm, but its effects are limited. The most effective mechanism takes place when the phase velocity of the dominant waves approaches the wind speed (see Komen et al, 1994 for a full description of the related physics). This is referred to as the diode effect, and it appears after the sea is sufficiently developed.

Fig.4 shows the growth curves obtained with a mean wind speed of 15 m/s and a gustiness level σ=0.25. With respect to the non-gusty reference run, the flip-flop curve illustrates well the pure effect of gustiness, with an enhanced growth. The no-coherence run oscillates around the flip-flop one, the differences representing the randomness of the input wind. However, due to the lack of coherence in time (α=0), the oscillations of the wave height are rather limited. Things change dramatically when coherence is considered. This implies a tendency of the wind speed to remain in a certain range, hence the wave height oscillations are much increased, with large positive and negative extremes, still around the same average, enhanced, growth curve. So we see that the effect of coherence in time is to superimpose to the pure enhancement due to gustiness some oscillations whose amplitude depend on the coherence between sequential wind values. It is important to note that these oscillations are not deterministic, but they can be described only in statistical terms. This will be further discussed in the next section.

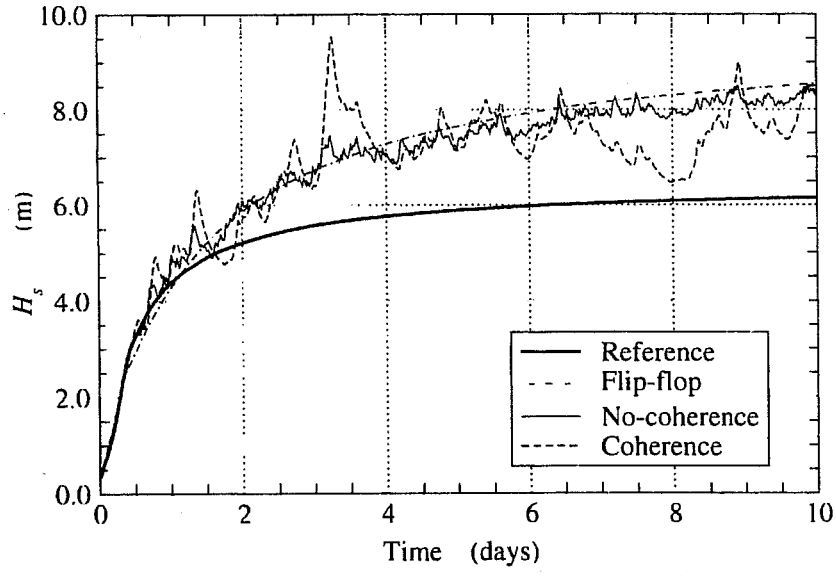

Fig 4 Growth curves for a single point wave model for non-gusty (reference) and gusty conditions.

The wind vectors oscillate not only in modulus, but also in direction (see, e.g., Ponce de Leon and Ocampo-Torres, 1998). Wind records suggest that the related σ_θ is rather limited, with values less than 10°, and an average values σ_θ= 4°. A series of tests was carried out, with an organisation similar to that for wind speed, using σ_θ=10°. We found that the main effect is a decrease of the significant wave height H_s by 1%. A much smaller reduction was found for σ_θ=4°. Therefore the problem was not further considered.

3. Practical applications – gustiness

To check the implications of gustiness for practical applications two long term hindcasts have been carried out, one in the Mediterranean Sea, representative of the enclosed basins, and another one in the North Atlantic ocean, representative of the oceanic large scale. The set-up was similar to what described in the previous section, the random sequence being different and independent for each grid point. The six hourly surface wind speed, linearly interpolated for intermediate times, was retrieved from the ECMWF archive. From here we derived also the air and sea surface temperatures used to evaluate, with (2), the level of gustiness at each time and location.

3.1 Mediterranean Sea

With a relatively warm water distribution and frequent spells of cold air from the North, the Mediterranean is characterised by air-sea instability, hence by gustiness. The period chosen for the hindcast goes from October 1993 to March 1994. It was chosen for the large number of storms that occurred in the basin. At this time the operational version of the ECMWF meteorological model was T213, with a spectral resolution of 95 km (Simmons, 1991). The WAM model resolution was 0.25 degree, with an integration time step of 15 minutes. Repetitive comparison with measured data, both of wind speed and of the derived wave height fields (see, e.g., Mork and Barstow, 1998, and Cavaleri and Bertotti, 1997) shows that the T213 surface wind speeds, hence the wave heights, are strongly underestimated in the Mediterranean Sea. Therefore, for the purpose of this paper, there is no interest in comparing the model results, without and with gustiness, against measured data. Rather, to check directly how much gustiness can affect the local wave fields, we have chosen to do some runs where the level of gustiness was constant and spatially uniform. Fig.5 shows the resulting U_{10} and H_s at Alghero, on the North-West corner of Sardinia (Fig.1) for a nine day period. Beside the reference non-gusty curve, the lower panel shows the H_s time series also for the cases σ= 0.10 and 0.25. The interesting point is the rather limited effects of gustiness on wave height. There is hardly any effect for σ=0.10, and only a limited one for σ=0.25, particularly when comparing the results with those in Fig.4. There is a basic difference between the two series of tests that is essential to understand. In the single point tests we have an infinite ocean with spatially uniform conditions. Hence, when, due to the random oscillations, U_{10} grows to higher values, this happens on the whole field. On the contrary, in nature the oscillations at the various grid points, if sufficiently far from each other, are practically independent. Given that wave heights are an integrated effect, in time and space, of the driving wind field, it is much more unlikely to reach in nature the extremes noted in Fig.4.

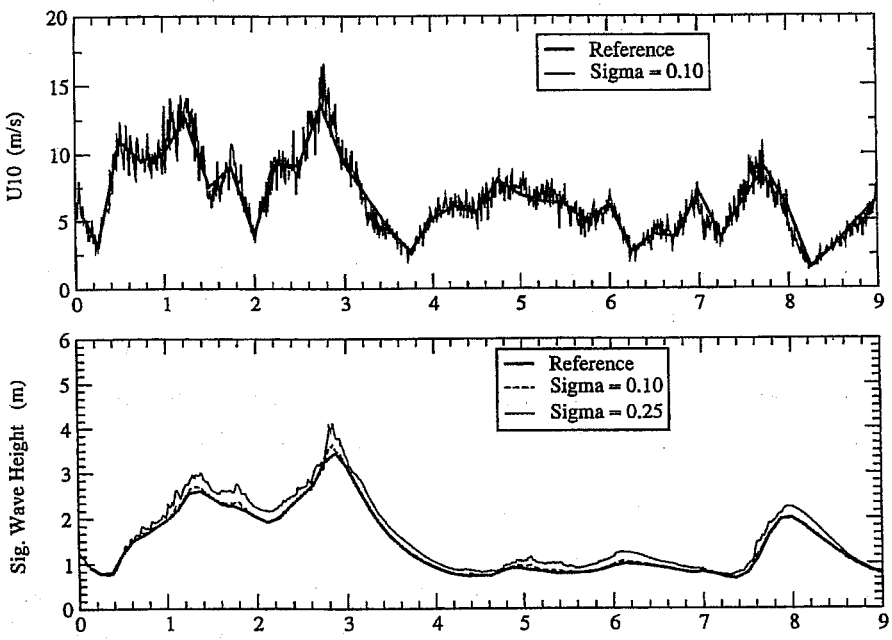

Fig 5 Upper panel: reference and gusty wind time series at Alghero, on the North-West side of Sardinia (see Fig.1). Lower panel: corresponding wave heights, for two different levels, 0.10 and 0.25, of gustiness.

There is another, purely physical, reason for the limited oscillation in Fig.5. We have pointed out that the diode effect, the basic mechanism for wave enhancement due to gustiness, is effective only when the sea is well developed, i.e. when the phase speed of the dominant wave-length becomes comparable to the wind

speed. In the Mediterranean Sea, and more in general in the enclosed basins, the fetch limitations prevent a sufficient development, hence the gustiness effects are limited.

3.2 North Atlantic ocean

The situation is obviously different in the open oceans, where the large fetches allow the development of very mature seas, and the consequent effect of gustiness. We have done a six month hindcast in the North Atlantic ocean, considering the area from 30 to 81 degrees North. The closed lower boundary excludes the presence of swell from the more southerly areas. However, most of the severe storms are from West or North-West, so for our purposes the implications of a closed grid are limited. The period considered is October 1999 – March 2000, when ECMWF had moved to the T319 version (abou 60 km resolution) of their meteorological model. The WAM model resolution was 1.0 degree, with a 15 minute integration time step.

Fig.6 shows the distribution of gustiness level during a severe storm, with σ values up to and larger than 20%. This is a typical case of north-westerly storm, with cold wind blowing over still relatively warm waters. Similar conditions are not the rule, hence the average long term effects of gustiness are limited. However, they represent well the cases when the combination of strong gustiness and extended fetches leads to a substantial enhancement of the otherwise "smooth" (non-gusty) generation. On the long term (a six month test period) the average increase of wave height due to gustiness varies between 10 and 18 cm. This is quite an interesting result, because this is the same order of magnitude of the present bias of the global WAM wave model at ECMWF.

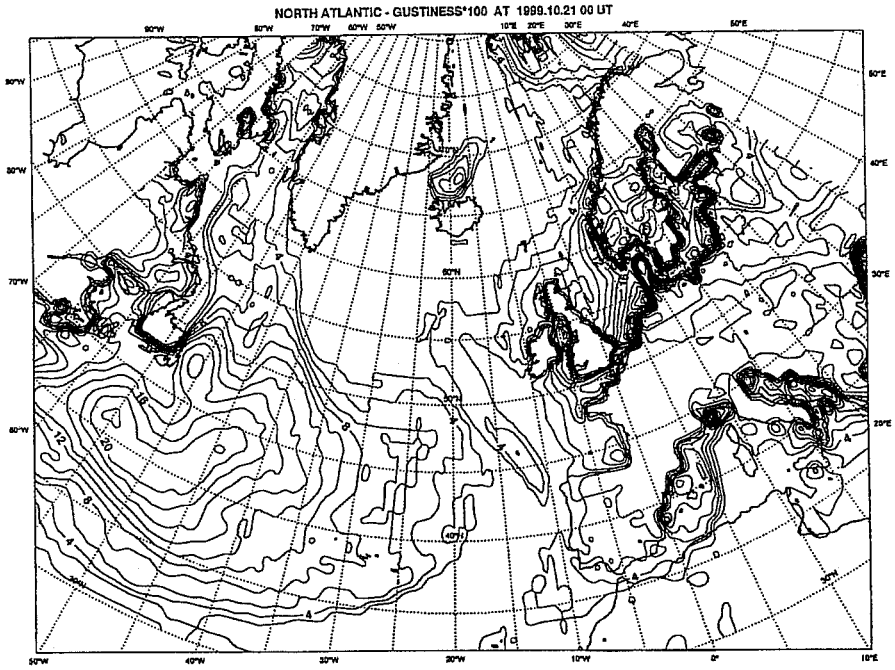

Fig 6 Distribution of gustiness level in the North Atlantic ocean.

On a local basis, in time and space, the increase can be much larger, up to one metre of average enhancement during a storm. Single local increases can be extreme, up to six metres in our test. This is associated with gustiness, so the single values can be considered only in statistical terms. Most likely a different realisation of the wind variability would have led locally to a quite different result. This aspect of the problem can be analysed with the ensemble approach. After choosing one storm, 16-21 December 1999, with west to north-westerly winds, we have hindcast it 50 times, each one with a different realisation of gustiness. Besides, two more runs have been done, using the flip-flop and no-coherence approaches described in the previous sections. The results are shown in Fig.7 for a point (60.5°N, 5.0°W) where buoy wave data are available.

This location, north of U.K., is partially shielded from the southern swell, hence the comparison is meaningful.

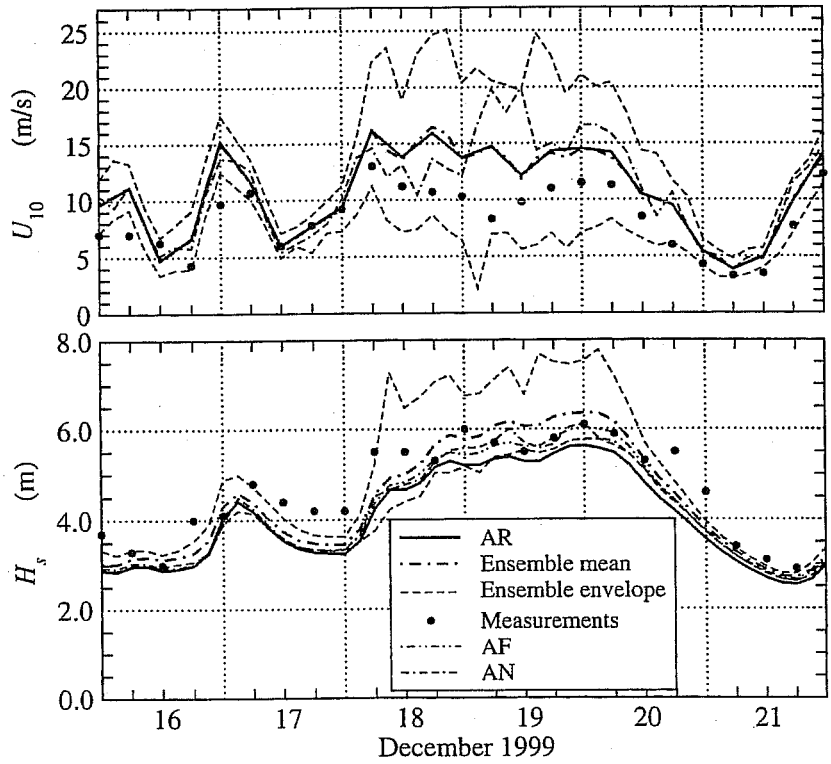

Fig 7 Upper panel: time series of wind speed during a storm in the North Atlantic ocean. The dashed line indicate the upper and lower limit values reached with 50 different realisations of gustiness. Lower panel: same as upper panel, but for wave height. See the text for a detailed explanation of the different curves.

The upper panel shows the wind history during the storm. Beside the undisturbed time series, we see the upper and lower borders of the values reached because of gustiness, the mean U_{10} values from the 50 gusty realisations (very close to the undisturbed values), and the no-coherence time series. The onset and termination of the gusty period are made evident by the large amplitude of the oscillations.

The effect on wave heights is displayed in the lower panel. Here too we have the undisturbed time series (AR), the flip-flop results (AF) and the no-coherence run (AN). All these results are larger than AR, and closer to the measured data (dots). The dashed lines are the upper and lower borders of the ensemble values, with their means being higher than the other (AR, AF, AN) runs. Note that almost all the H_s values, for each of the 50 realisations, are larger than those of the reference run. This is particularly true when the sea is well developed,, i.e. after the 18th, and the diode effect is fully active.

The question is how to handle randomness in practical applications. Obviously for the time being the ensemble approach is not acceptable. A solution is given by the study of the statistical distribution of the H_s ensemble values at each time when the results are available. Fig.8 shows the resulting average distribution, normalised with respect to the mean of the ensemble $\langle H_s \rangle$. R is the corresponding reference non-gusty value, N the no-coherence, F the flip-flop one. We have found that the F-R difference characterises the distribution, providing an estimate of the mean of the ensemble ($\langle H_s \rangle$-R ~ 2(F-R)) and of its standard deviation (=F-R). Clearly these estimates are rather approximate, but, on the sole basis of R and F, they give an indication of the probability of extreme values during a storm.

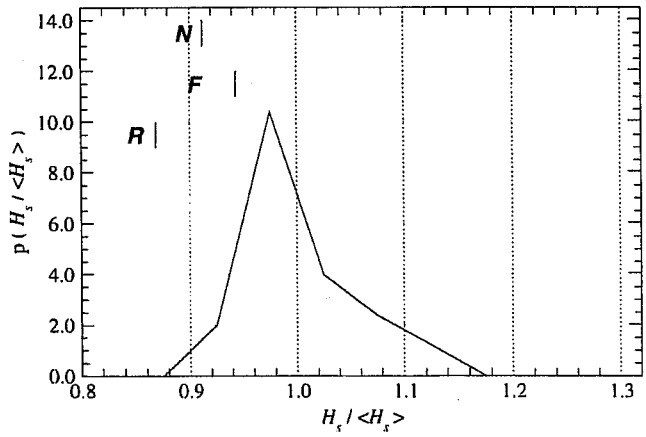

Fig 8 Average distribution of the H_s ensemble values in Fig.7, normalised with respect to the mean of the ensemble <H_s>. R, F, N show the corresponding reference, flip-flop and no-coherence values.

4. The effect of air density on wave growth

As we have mentioned in the first section, the air density ρ_{air} is usually considered as constant in wave modelling. At ECMWF the standard value is ρ_{air} = 1.225 kg/m^3. However, actual values vary appreciably from this reference, up to 10%. Given that the wind input to waves is directly proportional to ρ_{air}, its variability must have an effect on wave growth.

We have verified this with some single point tests, similar to those described in sect.2. The wind speed was fixed at 15 m/s, varying the air density according to the values shown in Fig.9. The figure reports also the resulting wave growth curves. As expected, H_s is larger (smaller) for larger (smaller) values of ρ_{air}. Note that, with respect to the results in sect.2, these results are more significant for practical applications. The air density shows a high degree of spatial correlation, hence the single point tests are quite representative of what we can expect in nature.

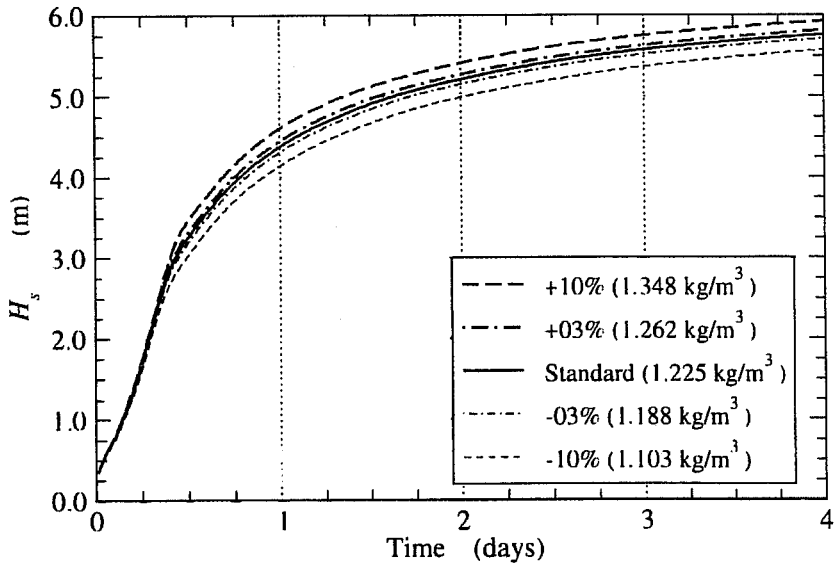

Fig 9 Growth curves of wave height for different values of the air density.

5. Practical applications – air density

For the tests with a variable air density we have made use of the same periods and areas used for gustiness (see sect.3). The wind fields were the ones from the ECMWF archive, while we have used the air temperature and humidity to derive its density values. As before, we discuss separately the results in the two areas.

5.1 Mediterranean Sea

The average effect of considering a variable air density is quite limited. This is because the average $<\rho_{air}>$ in the Mediterranean Sea is close (slightly lower) than the nominal value, hence changes in $<H_s>$ are minor, of order 1 cm. There are cases when a cold burst from the North, typically a mistral storm, is characterised by higher ρ_{air} values. In these cases we have found differences up to +35 cm. A similar, negative, value has been for southerly storms, where the warmer air leads to a lower density.

5.2 North Atlantic ocean

The analysis of the fields shows that the North Atlantic is characterised, on the average, by air density values larger than the nominal one. Fig.10 shows the distribution of $<\rho_{air}>$ during January 2000. The isolines show the first two decimal digits; i.e. 24 = 1.240 kg/m^3. We see that differences up to 6% are present, on the average, on the open sea, and much larger values appear, expectably, moving to North. The distribution reflects the presence of frequent west or north-westerly storms, bringing with them large masses of cold, heavy air.

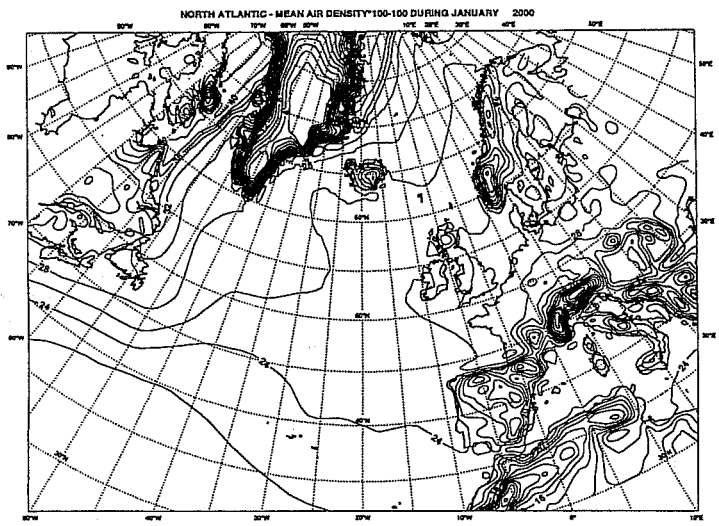

Fig 10 Distribution of average air density in the North Atlantic ocean during January 2000. E.g., 24=1.240 kg/m^3.

The six month wave hindcast has shown an average increase of H_s of about 10 cm, with single positive differences larger than one metre. Fig.11 provides the distribution of the maximum increase for each grid point throughout the six month hindcast.

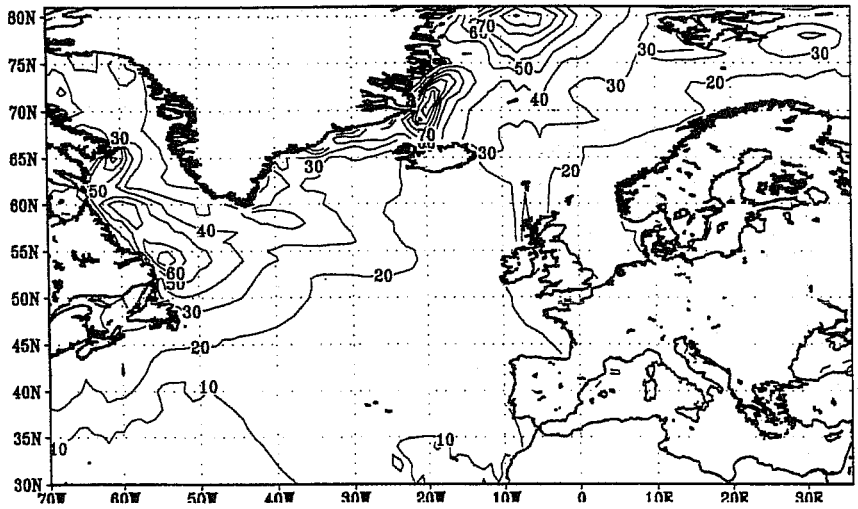

Fig 11 Maximum increases, in centimetres, of the wave heights in the North Atlantic as a result of the use of the correct air density. The period is October 1999 – March 2000.

6. Conclusions

Gustiness has limited effects, on the average, in the enclosed basins, because the limited fetches prevent a sufficient development of the sea conditions for the onset of the diode effect. The nonlinearity of u_* with respect to U_{10} has only marginal implications. Local enhancements are possible due to the randomness of the input wind fields.

The effects are much larger in the open oceans, where the large fetches allow a sufficient development of the sea conditions. A severe storm can lead to an average increase of the wave height field of the order of one metre. Much large increases are locally possible due to randomness. Gustiness must be expected in areas open to bursts of cold air, particularly in the Fall, when the sea water is still relatively warm. As a gusty storm is not the rule, the average long term increase of the wave heights in the North Atlantic is between 10 and 20 cm. This difference is comparable to the present bias of the ECMWF global wave model.

The implications of a variable air density should be taken into consideration in wave modelling, also in view of the limited effort required for its implementation. The overall effect is very limited in the Mediterranean Sea, where the density is on the average close to the nominal value. Single differences, both positive and negative, up to 35 cm have been found. The implications are much larger in the North Atlantic, where the air density in the winter months is usually larger than the nominal value. We have found an average increase of the significant wave heights of about 10 cm, with single values up to one metre.

We have explored the interaction between gustiness and a variable air density by hindcasting the 16-21 December 1999 storm, first with one particular realisation of gustiness, then with a variable air density, and finally with both the processes at work. The results, expressed as differences with respect to the reference run (no gustiness, constant ρ_{air}), are given in Fig.12. The interesting aspect is that the combined run leads to H_s values larger than the sum of the two single effects. This is because the higher wave heights derived, in this case, from a variable air density enhance the gustiness effect. An opposite result should be expected for the cases when ρ_{air} is lower than the nominal values.

The theories presently available do not justify the large levels of gustiness experienced in the field. For the tests described in this paper we have resorted to an empirical relationship between the level of gustiness and

the local air-sea temperature differences. A different approach has been followed for the implementation at ECMWF (reported by Saleh Abdalla).

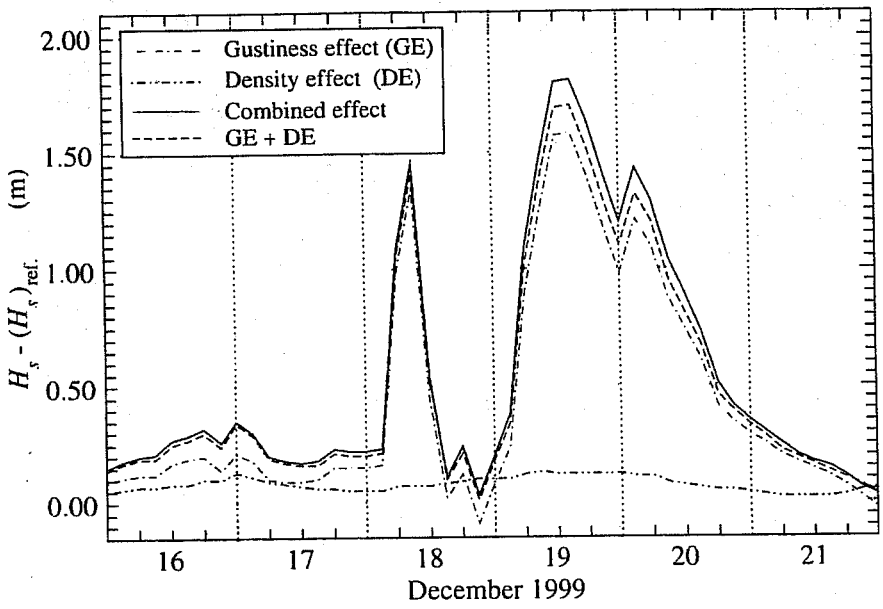

Fig 12 Increase of wave height at one specific point due to the introduction of gustiness, correct air density, and the coupled use of the two effects.

A key point associated to gustiness is the statistical character of the oscillations around the smooth enhanced growth curve, represented in Fig.4 by the flip-flop line. Their distribution has been studied with the ensemble approach. It has been found that its characteristics (mean value and width of the distribution) can be approximately derived using the reference and the flip-flop runs only.

Acknowledgements

The present paper is based on the work done with dr. Saleh Abdalla during his six month staying at ISDGM, in Venice. Dr. Saleh Abdalla is presently working at ECMWF.

References

Bauer, E., and R.Weisse, Influence of quasi-realistic high-frequency wind variability on wave modelling in the North Atlantic, *Journal of Geophysical Research*, **105**, No.C11, pp.26,179-26,190, 2000.

Box, G.E.P. and G.M.Jenkins, *Time Series Analysis, Forecasting and Control*, 553 pp., Holden Day, S. Francisco, 1970.

Cavaleri, L., The oceanographic tower *Acqua Alta* - activity and prediction of sea states at Venice, *Coastal Engineering*, 39, pp.29-70, 2000.

Cavaleri, L. and G.Burgers, Wind gustiness and wave growth, *KNMI-Preprints*, 92-18, 38pp., Koninklijk Nederlands Meteorologisch Instituut, De Bilt, The Netherlands, 1992.

Cavaleri, L. and L. Bertotti, In search of the correct wind and wave fields in a minor basin, *Monthly Weather review*, **125**, No.8, pp.1964-1975, 1997.

Komen, G.J., L. Cavaleri, M. Donelan, K. Hasselmann, S. Hasselmann and P.A.E.M. Janssen, *Dynamics and Modelling of Ocean Waves*, 532pp., Cambridge University Press, Cambridge, UK, 1994.

Monahan, H.H. and P. Armendariz, Gust factor variations with height at atmospheric stability, *Journal of Geophysical Research*, **76**, pp.5807-5818, 1971.

Mork, G. and S.F.Barstow, Comparison of WAM estimates of H_s with TOPEX/POSEIDON altimeter data in the Mediterranean Sea; a comparison of low and high resolution wind models, OCN Report R-98019, 152pp, 1998.

Ponce de Leon, S., and F.J.Ocampo-Torres, Sensitivity of a wave model to wind variability, *J.Geoph.Res.*, **103**, No.C2, pp.3179-3201, 1998.

Sethuraman, S., Atmospheric turbulence and storm surge due to Hurricane Belle (1976), *Monthly Weather Review*, **107**, pp.314-321, 1979.

Simmons, A., Development of the operational 31-level T213 version of the ECMWF forecast model, *ECMWF Newsletter*, No.56, pp.3-13, 1991.

Smith, S.D., K.B. Katzaros, W.A. Oost and P.G. Mestager, Two major experiments in the humidity exchange over the sea (HEXOS) program, *Bulletin of the American Meteorological Society*, **71**, pp.161-172, 1990.

WAMDI Group, The WAM model – a third generation ocean wave prediction model, *Journal of Physical Oceanography*, **18**, pp.1775-1810, 1988.